PHYSICAL REVIEW E **00**, 000100(R) (2015)

# Temperature inversion of the thermal polarization of water

Jeff Armstrong[1,*] and Fernando Bresme[1,2,†]
[1]*Department of Chemistry, Imperial College, London SW7 2AZ, United Kingdom*
[2]*Department of Chemistry, Norwegian University of Science and Technology, Trondheim, Norway*
(Received 7 August 2015; revised manuscript received 5 December 2015; published xxxxxx)

Temperature gradients polarize water, a nonequilibrium effect that may result in significant electrostatic fields for strong thermal gradients. Using nonequilibrium molecular dynamics simulations, we show that the thermal polarization features a significant dependence with temperature that ultimately leads to an inversion phenomenon, whereby the polarization field reverses its sign at a specific temperature. Temperature inversion effects have been reported before in the Soret coefficient of aqueous solutions, where the solution changes from thermophobic to thermophilic at specific temperatures. We show that a similar inversion behavior is observed in pure water. Microscopically, the inversion is the result of a balance of dipolar and quadrupolar contributions and the strong temperature dependence of the quadrupolar contribution, which is determined by the thermal expansion of the liquid.

DOI: 10.1103/PhysRevE.00.000100 PACS number(s): 65.20.De, 05.70.Ln, 44.10.+i, 61.20.Ja

Materials exposed to thermal gradients exhibit nonequilibrium responses that arise from the coupling of several fluxes [1]. In metals and semiconductors, thermal gradients can induce electric currents. This "thermoelectric effect" was discovered by Seebeck in 1821, and provides a physical principle to harvest waste heat [2]. Ludwig discovered that thermal gradients can induce mass separation too [3], an effect that was investigated systematically by Soret in aqueous solutions [4]. The Soret effect has been used to direct the motion of colloidal particles [5,6] and separate binary mixtures [7]. More generally, it has been shown that thermal gradients can drive the motion of thermal machines [8] and to induce Casimir-like forces on two confining walls maintained at different temperatures [9]. Furthermore, the relevance of thermal gradients in the rate of biochemical reactions has been noted [10].

Many experiments have been devised to understand and quantify the Soret effect in aqueous suspensions and fluid mixtures [11–13]. Those works have motivated the development of theoretical approaches to predict the magnitude of the Soret effect [12,14,15]. These are very important advances that provide an understanding of the salt and temperature dependence of the Soret effect in some situations [15]. Strong deviations between experiment and theory have been reported in other works as well [16]. Hence, a full predictive theory of thermodiffusion and thermophoresis is still an outstanding and desirable objective. Such a theory should predict the temperature inversion of the Soret coefficient, namely, the temperature at which the solutions change from thermophobic to thermophilic or vice versa [16–21]. It has been noted that this inversion temperature is similar for a variety of systems [17,18,18,21]. Further, theoretical approaches should take into account the so-called nonionic contribution to the Soret effect, which has been highlighted in experiments of protein solutions [18].

We recently discovered that thermal gradients can induce a thermopolarization (TP) field in water [22]. Using nonequilibrium thermodynamics (NET), we established that the TP effect can arise from a coupling of the displacement current $\partial\mathbf{P}/\partial t$ and the heat flux $\mathbf{J}_q$. An equation for the TP field, $\mathbf{E}$, was derived [22],

$$\mathbf{E} = \left(1 - \frac{1}{\varepsilon_r}\right)\frac{L_{pq}}{L_{pp}}\frac{\nabla T}{T}, \tag{1}$$

where $\varepsilon_r$ is the fluid dielectric constant, $\nabla T$ the thermal gradient, $T$ the temperature, and $L_{pq}/L_{pp}$ the ratio of phenomenological coefficients, where $L_{pq}$ measures the TP coupling. Using computer simulations and different water models, we found that the TP field changes linearly with the thermal gradient, as predicted by Eq. (1) [22–24]. We show in this Rapid Communication that the TP field features a strong temperature dependence and reverses sign at a specific temperature. Further, we provide a microscopic interpretation of the TP field inversion, which advances our microscopic understanding of TP effect, beyond the phenomenological treatment of NET.

We have performed nonequilibrium molecular dynamics (NEMD) simulations (see, e.g., Ref. [22]). Two geometrical regions were defined, in which the temperature is controlled by rescaling velocities every time step. The molecules outside the thermostatting regions move according to Newtonian dynamics. We computed the temperature profile and the TP field locally by dividing the simulation box into bins of width 0.7 Å. For analysis purposes we discarded the bins next to the thermostats (typically 10). All the computations were performed with the extended simple point charge (SPC/E) model of water [25], and the electrostatic interactions and TP fields were computed using the three-dimensional particle-particle particle-mesh (PPPM) Ewald summation method [26] with "tin-foil" boundary conditions [24]. Our longest simulation involved a 126 ns trajectory. To ensure the system reached the stationary state, we discarded the first 2 ns of the trajectory. The total electric field was computed *on the fly* every ten steps, while the calculations of the dipolar and quadrupolar contributions were performed externally. The trajectories were integrated using the velocity-Verlet algorithm with a time step of 2 fs using the parallel code LAMMPS [27]. For each of these systems investigated in this work, the density required in order to achieve a given pressure $P$ was determined via an $NPT$ simulation using the Nosé-Hoover barostat. The systems were allowed to equilibrate for 4 ns. After equilibration, a subsequent 4 ns run was used to determine the average density

*j.armstrong@imperial.ac.uk
†f.bresme@imperial.ac.uk

 

TABLE I. Hot and cold thermostat temperatures ($T_{hot}$ and $T_{cold}$) employed in the NEMD runs, box dimensions ($L_x$, $L_y$, and $L_z$), average pressure $P$, and total simulation time ($\tau$) of each simulation. Simulations used to calculate the dipolar and quadrupolar contributions have been indicated with an asterisk.

| $T_{cold}$ (K) | $T_{hot}$ (K) | $L_x = L_y$ (Å) | $L_z$ (Å) | $P$ (bar) | $\tau$ (ns) |
|---|---|---|---|---|---|
| 240 | 320 | 35.35 | 35.35 | 414 | 105 |
| 240 | 320 | 35.35 | 35.35 | 414 | 126* |
| 400 | 500 | 37.07 | 37.07 | 364 | 80 |
| 350 | 550 | 37.07 | 37.07 | 367 | 80* |
| 500 | 600 | 27.23 | 81.69 | 312 | 31 |
| 500 | 600 | 39.27 | 39.27 | 323 | 57* |

of water at the desired average temperature of the NEMD run. The short range Lennard-Jones interactions were truncated in all cases at 11 Å. Information detailing all of the NEMD simulations performed is compiled in Table I.

We show in Fig. 1 the TP field for the three temperature intervals studied in this work at ∼350 bars. The pressure deviates at most by ∼±50 bars between the studied systems. We found that these pressure fluctuations have a minor impact on the equation of state of SPC/E water (see Fig. 2).

The electric field in the direction of the heat flux was calculated from the integral of the charge density,

$$E(z) = \frac{1}{\varepsilon_0}\int_0^z \rho_q(z')dz', \tag{2}$$

where $\varepsilon_0$ is the vacuum permittivity, $\rho_q(z) = \sum_{i=1}^{N} \delta(z - z_i)q_i/A$ is the charge density at $z$, $A$ is the box cross sectional area, $q_i$ represents the charge of a given atom, and the integration runs from the box origin set at "0." The sum runs over all the charges in the system $N$. We find that the scaled TP field, $E/\nabla T$, is negative at high average temperatures (450 and

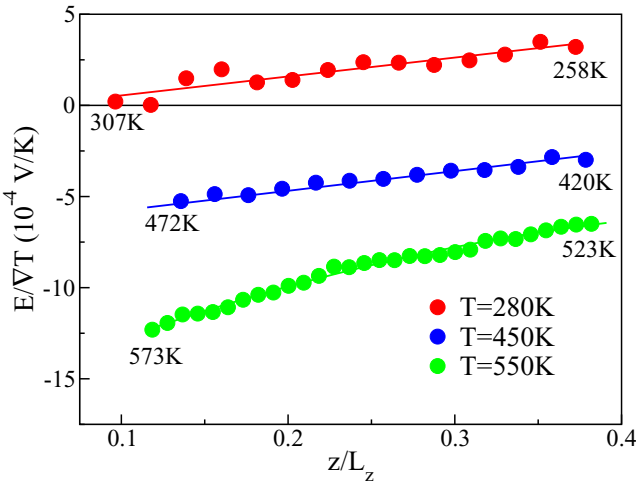


FIG. 1. (Color online) The scaled TP field $E/\nabla T$ along the simulation box at different average temperatures, 280, 450, and 550 K, and absolute temperature gradients of 4.53, 5.4, and 2.45 K/Å, respectively. The numerical labels indicate the temperature in the simulation box at the specific points. The solid lines are a guide to the eye.

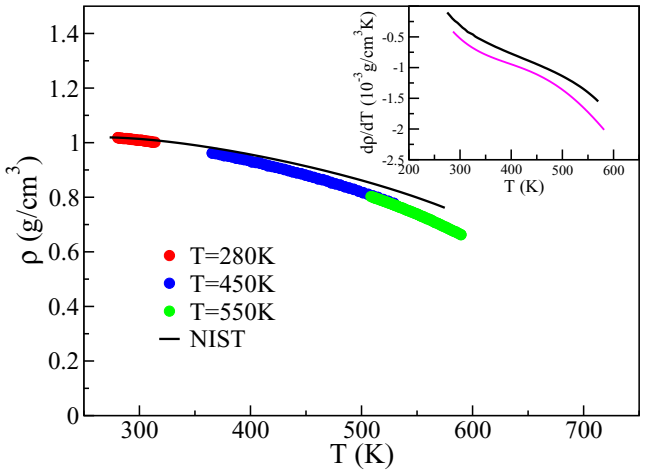


FIG. 2. (Color online) The main plot shows the equation of state as calculated from the combined simulation for average temperatures 280, 450, and 550 K. The black line represents the experimental equation of state for the same pressure taken from the NIST database. The inset shows $d\rho/dT$ (magenta), which is the key quantity in our analytical calculation of the total electric field, and again the equivalent experimental value taken from NIST is represented in black.

550 K), while it reverses sign at lower average temperatures (280 K), becoming positive.

We have previously shown that the TP field changes linearly with the thermal gradient, as predicted by NET (see Refs. [22,24]), indicating that the nonequilibrium response is within the linear regime. This linear response is compatible with the inequality $|\nabla T|T^{-1}L \ll 1$ [28], which is fulfilled in our computations (∼$10^{10}$ K/m, thermal transport mean free path, ∼$10^{-10}$ m, and simulation temperatures, ∼240–600 K).

We have used Eq. (1) to estimate the strength of the TP effect. We define the thermo-polarization coefficient $S_{TP} \equiv E/\nabla T = \left(1 - \varepsilon_r^{-1}\right) L_{pq}(L_{pp})^{-1}T^{-1}$, which is similar to the Seebeck coefficient in thermoelectric phenomena. For our systems, $S_{TP}$ changes significantly in magnitude and sign (+400 to −1300 $\mu$V/K), with values similar to the Seebeck coefficient of aqueous and nonaqueous electrolytes, ∼10–$10^4$ $\mu$V/K. [16,29,30]. Additional simulations at different pressures (see Fig. 4) show that $S_{TP}$ is fairly independent of the pressure at ∼300 K, with $S_T \sim 100$ $\mu$V/K, which is similar to the Seebeck coefficient of common salts at infinite dilution (50 and 35 $\mu$V/K, for NaCl and KCl, respectively) [29].

We have shown above the existence of a sign reversal in the TP field of water. For the system and model (SPC/E) investigated in this work, the sign inversion appears at ∼320 K for a wide range of pressures. We now consider the microscopic origin of the inversion phenomenon. We have focused our attention on the polarization field. The TP electrostatic field computed from the integral of the charge density [see Eq. (2)] can also be obtained from the expansion of the charge density in terms of dipolar, quadrupolar, and higher order terms. We consider the projection of these terms along the direction of the heat flux $z$,

$$\rho_q(z) = -\frac{d}{dz}\left(P_z(z) - \frac{dQ_{zz}(z)}{dz} + \cdots\right), \tag{3}$$

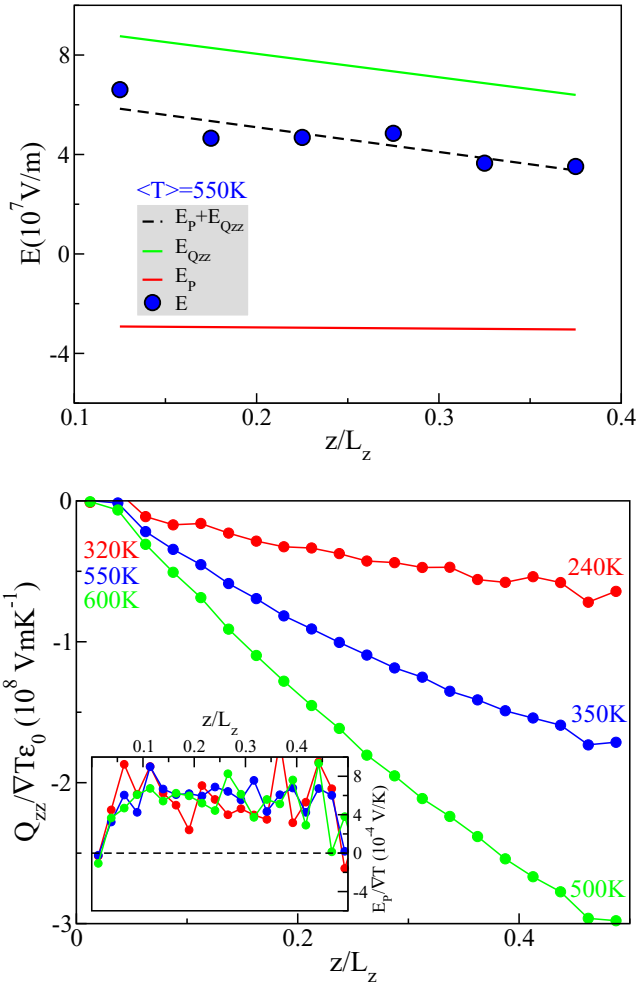


FIG. 3. (Color online) Top: The dipolar ($E_p$) and quadrupolar ($E_{Q_{zz}}$) contributions to the electric field obtained from Eqs. (6) and (7). The sum of these contributions (dashed line) is compared with the electric field obtained from the integration of the charge density [Eq. (2)] (circles). The average temperature of this simulation was 550 K and the hot thermostat was situated at $z = 0$. Bottom: The variation of the $E_P/\nabla T$ (inset) and $Q_{zz}/\varepsilon_0\nabla T$ (main plot) along the simulation box for the systems presented in Fig. 1 are shown. The values for $Q_{zz}$ have been shifted such that $Q_{zz} = 0$ at $z = 0$, in order to facilitate the comparison of the systems corresponding to different temperature intervals. Maximum and minimum temperature labels are also shown.

where we have not written explicitly the octupolar and higher order terms. The dipolar, $P_z$, and the quadrupolar, $Q_{zz}$, contributions can be calculated from a sum over the number of molecules $N_m$ [31,32],

$$P_z(z) = \frac{1}{A}\left\langle \sum_{i=1}^{N_m} \delta(z - z_i) \left[ \sum_{j=1}^{j\in m} q_{j,m} z_{j,m} \right] \right\rangle, \quad (4)$$

$$Q_{zz}(z) = \frac{1}{A}\left\langle \sum_{i=1}^{N_m} \delta(z - z_i) \left[ \frac{1}{2} \sum_{j=1}^{j\in m} q_{j,m} z_{j,m}^2 \right] \right\rangle, \quad (5)$$

where the brackets indicate an ensemble average, and $z_i$ is the reference position of the molecule, defined by the coordinates of the oxygen atom in the water molecule. $z_{j,m}$ is the position of atom $j$ in molecule $m$ relative to the reference position of that molecule, and $q_{j,m}$ is the charge of site $j$ in molecule $m$. The molecular electrostatic field is given by

$$E_{\text{mol}}(z) = E_P(z) + E_{Q_{zz}}(z) \quad (6)$$

$$= \frac{-1}{\varepsilon_0}\int_0^z \frac{dP_z(z')}{dz'}dz' + \frac{1}{\varepsilon_0}\int_0^z \frac{d^2Q_{zz}(z')}{dz'^2}dz', \quad (7)$$

which is equivalent to Eq. (2) provided the octupolar and higher order terms can be neglected. We demonstrate in Fig. 3 that these terms can indeed be neglected by showing that the sum of the dipolar and quadrupolar terms is in excellent agreement with the field obtained from the atomic charges [Eq. (2)]. The analysis of Fig. 3 shows that the dipolar contribution $E_P/\nabla T$ is positive and features no significant dependence with temperature, while the quadrupolar contribution $E_{Q_{zz}}/\nabla T$ is negative and dominant, showing at the same time a strong dependence with temperature (see Fig. 3). The fact that $E_P$ and $E_{Q_{zz}}$ have opposite signs immediately suggests that these two contributions may cancel each other, leading, possibly, to a zero TP field. Our simulations show that the dipolar term provides a static contribution to the TP field in all cases, while the quadrupolar term provides an opposing field and accounts for the strong temperature variation of the field.

The sign of $P_z$ at the three temperatures investigated here indicates that the water molecules orient preferentially with the dipole pointing towards the cold region, both above and below the inversion temperature, hence from the dipole orientation perspective, SPC/E water is thermophobic for the thermodynamic states investigated.

We have shown so far that the quadrupolar term is responsible for the largest temperature changes observed in the TP field. We explore now the physical origin of this observation. $Q_{zz}$ may change either as a response to changes in the water density (driven by the thermal expansion of the fluid under the thermal gradient), and/or by a modification of the orientational distribution of the water molecules. To understand the origin of the variation in the quadrupolar term, we calculated $Q_{zz}$ for a homogeneous bulk water system at one of the thermodynamic states studied above ($T = 280$ K). We assess possible changes in the orientation probability distribution by calculating the quadrupole contribution per unit density, i.e., $Q_{zz\rho} = Q_{zz}/\rho$. If $Q_{zz\rho}$ is the same in both the NEMD cases and the equilibrium case, then the observed variation of $Q_{zz}$ would be dominated by the thermal expansion undergone by the fluid as a response to the temperature gradient. We show in Fig. 4 for one of the simulated pressures that $Q_{zz\rho}$ agrees within 0.5% deviation with the equilibrium simulation data. Hence, the variation of the quadrupolar field can be correlated with the thermal expansion of the fluid. We have used this notion to write the phenomenological equation

$$E_{\text{phen}} = \nabla T\left[\left|\frac{E_P}{\nabla T}\right| - \frac{\alpha\rho Q_{zz\rho}}{\varepsilon_0}\right], \quad (8)$$

where the first term inside the brackets is the absolute value of the temperature gradient normalized dipolar field, which was

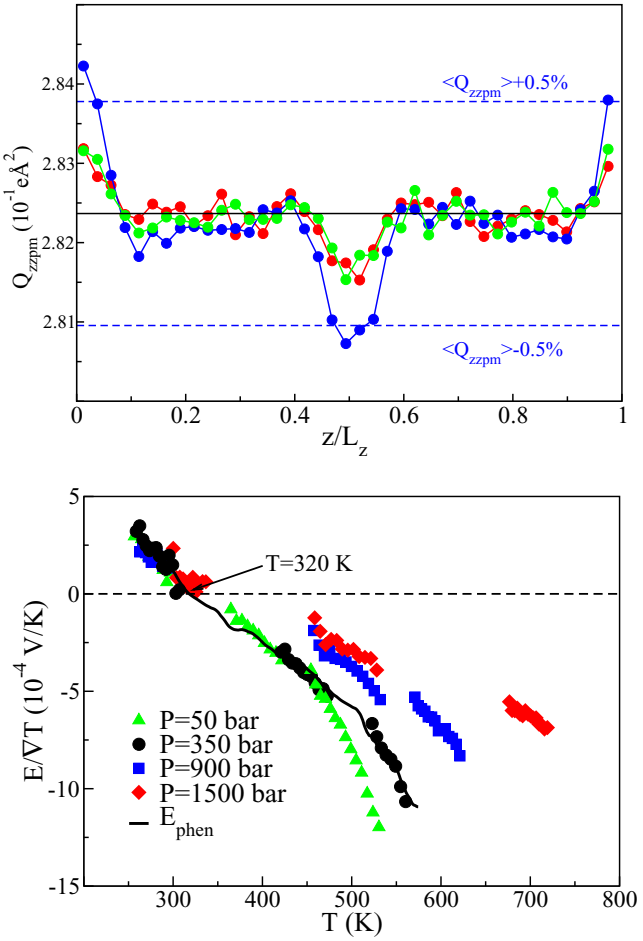


FIG. 4. (Color online) Top: The figure shows $Q_{zz\rho}$ along the simulation cell for the average NEMD run temperatures, 280 K (red), 450 K (blue), and 550 K (green). The average value of $Q_{zz\rho}$ for an equilibrium simulation at the same pressure in the NEMD simulations, and temperature 280 K is shown (solid line). The dashed lines indicate 0.5% deviations from the equilibrium value. Bottom: Temperature variation of $E/\nabla T$ for different isobars obtained from NEMD simulations (symbols). The solid line shows $E_{\text{phen}}/\nabla T$ calculated with Eq. (8) for the 350 bar isobar.

found to be approximately temperature independent within the temperature range studied, and $\alpha = -1/\rho(\partial\rho/\partial T)_P$ is the isobaric thermal expansion. We show in Fig. 4 that Eq. (8) very accurately reproduces the computed TP field, and features the sign inversion around 320 K. Computations at different pressures further support the notion that the thermal expansion of the fluid plays an important role in the TP effect, with a weaker change in the TP for higher pressures due to the reduced thermal expansion.

In summary, we have shown that the thermal polarization of water reverses sign at a specific temperature. We show that the inversion results from the balance of dipolar and quadrupolar contributions to the TP field, and the strong temperature dependence of the latter contribution, which is determined by the thermal expansion of water. We have proposed a phenomenological equation that accurately reproduces the variation of the TP field with temperature. It is interesting that previous experiments of protein solutions have noted that the nonionic contribution to the Soret coefficient features a strong correlation with the thermal expansion of water [33]. This observation resembles the strong dependence of the TP field with the thermal expansion [Eq. (8)]. Further work to establish a possible connection between these two observations is necessary.

The TP is a coupling effect and it therefore contributes to the heat flux. This suggests a possible experimental verification. By investigating a sample subjected to an oscillating electrostatic field, one would observe a heat flux for $S_{\text{TP}} \neq 0$, while no heat flux would be observed at the inversion temperature $S_{\text{TP}} = 0$. Our work highlights the potential relevance of the TP field in determining the nonequilibrium response of aqueous solutions under thermal gradients, and calls for an examination of the role that this field may play in determining the Soret and Seebeck coefficients of aqueous solutions.

We thank the EPSRC-UK (EP/J003859/1) and NFR (Project No. 221675) for financial support. We acknowledge the Imperial College High Performance Computing Service for providing computational resources. F.B. would like to thank the EPSRC for support via the award of a Leadership Fellowship.

[1] S. de Groot and P. Mazur, *Nonequilibrium Thermodynamics* (Dover, New York, 1984).
[2] G. Snyder and E. Toberer, Nat. Mater. **7**, 105 (2008).
[3] C. Ludwig, Sitzungsber. Akad. Wiss. Wien, Math.-Naturwiss. Kl., Abt. 1 **20**, 539 (1856).
[4] Ch. Soret, Arch. Sci. Phys. Nat., Genéve **2**, 48 (1879).
[5] H.-R. Jiang, H. Wada, N. Yoshinaga, and M. Sano, Phys. Rev. Lett. **102**, 208301 (2009).
[6] H.-R. Jiang, N. Yoshinaga, and M. Sano, Phys. Rev. Lett. **105**, 268302 (2010).
[7] A. Lervik and F. Bresme, Phys. Chem. Chem. Phys. **16**, 13279 (2014).
[8] M. Yang and M. Ripoll, Soft Matter **10**, 1006 (2014).
[9] T. R. Kirkpatrick, J. M. Ortiz de Zárate, and J. V. Sengers, Phys. Rev. Lett. **115**, 035901 (2015).
[10] P. Baaske, F. Weinert, S. Duhr, K. Lemke, M. Russel, and D. Braun, Proc. Natl. Acad. Sci. USA **104**, 9346 (2007).
[11] A. Würger, Phys. Rev. Lett. **101**, 108302 (2008).
[12] S. Duhr and D. Braun, Phys. Rev. Lett. **96**, 168301 (2006).
[13] M. Reichl, M. Herzog, A. Götz, and D. Braun, Phys. Rev. Lett. **112**, 198101 (2014).
[14] C. Debuschewitz and W. Köhler, Phys. Rev. Lett. **87**, 055901 (2001).
[15] K. Eslahian, A. Majee, M. Maskos, and A. Würger, Soft Matter **10**, 1931 (2014).
[16] S. Putnam, D. Cahill, and G. Wong, Langmuir **23**, 9221 (2007).
[17] S. Wiegand, J. Phys.: Condens. Matter **16**, R357 (2004).

[18] R. Piazza and A. Parola, J. Phys.: Condens. Matter **20**, 153102 (2008).
[19] P. Kolodner, H. Williams, and C. Moe, J. Chem. Phys. **88**, 6512 (1988).
[20] G. Wittko and W. Köhler, Europhys. Lett. **78**, 46007 (2007).
[21] F. Römer, Z. Wang, S. Wiegand, and F. Bresme, J. Phys. Chem. B **117**, 8209 (2013).
[22] F. Bresme, A. Lervik, D. Bedeaux, and S. Kjelstrup, Phys. Rev. Lett. **101**, 020602 (2008).
[23] J. A. Armstrong and F. Bresme, J. Chem. Phys. **139**, 014504 (2013).
[24] J. A. Armstrong, C. Daub, and F. Bresme, J. Chem. Phys. **143**, 036101 (2015).
[25] H. J. C. Berendsen, J. R. Grigera, and T. P. Straatsma, J. Phys. Chem. **91**, 6269 (1987).
[26] T. Darden, D. York, and L. Pedersen, J. Chem. Phys. **98**, 10089 (1993).
[27] S. Plimpton, J. Comput. Phys. **117**, 1 (1995).
[28] E. G. D. Cohen and R. L. Merlino, J. Comput. Theory Trans. **43**, 3 (2014).
[29] J. N. Agar, C. Y. Mou, and J. L. Lin, J. Phys. Chem. **93**, 2079 (1989).
[30] M. Bonetti, S. Nakamae, M. Roger, and P. Guenoun, J. Chem. Phys. **134**, 114513 (2011).
[31] J. Glosli and M. Philpott, Electrochim. Acta **41**, 2145 (1996).
[32] M. Wilson and A. P. A. Pohorille, J. Chem. Phys. **90**, 5211 (1989).
[33] S. Iacopini, R. Rusconi, and R. Piazza, Eur. Phys. J. E **19**, 59 (2006).